JMEPEG (2019) 28:273–277
https://doi.org/10.1007/s11665-018-3832-6

1059-9495/$19.00

Performance of Nd-Fe-B Magnets Fabricated by Hot Isostatic Pressing and Low-Temperature Sintering

Fang Yang, Haiying Wang, Li You, Alex A. Volinsky, Ce Zhang, Zhimeng Guo, and Yanli Sui

(Submitted April 12, 2018; in revised form September 17, 2018; published online December 17, 2018)

Magnetic properties and microstructure of Nd-Fe-B sintered magnets fabricated by hot isostatic pressing (HIP) were studied. For comparison, magnets were also fabricated by vacuum sintering. The density reached 7.58 g/cm^3 for the magnets HIP-sintered at 1123 K. The density of the magnets vacuum-sintered at 1123 K was much lower, which is of about 6.92 g/cm^3. While the density of magnets vacuum-sintered at 1318 K was the same as the HIP-sintered magnets, the sintering temperature was significantly decreased to 1123 K. In addition, the average grain size decreased from 9 to 6 μm, which has enhanced coercivity. Therefore, the coercivity increased from 1067.7 to 1238.5 kA/m, which is 16% higher than the vacuum-sintered magnets. HIP is a promising method to obtain high density and high coercivity Nd-Fe-B sintered magnets.

Keywords coercivity, grain refinement, hot isostatic pressing, Nd-Fe-B sintered magnets

1. Introduction

Due to excellent magnetic properties, Nd-Fe-B sintered magnets have attracted much attention in eco-friendly electrical applications, such as hybrid vehicles, electric vehicles, and wind power generators (Ref 1, 2). However, the relatively low coercivity cannot meet the growing requirements of elevated temperature operation ($>$ 473 K) (Ref 3). To overcome this problem, heavy rare earth (HRE) elements, such as Dy or Tb, are commonly introduced into the $Nd_2Fe_{14}B$ phase with a higher magnetic anisotropy field (Ref 4-6). Due to the scarcity and high cost, there is a strong demand to achieve high coercivity without using HRE elements. Among efforts to improve the coercivity of Nd-Fe-B sintered magnets without using HRE elements, one practical approach is to refine the grain size of the $Nd_2Fe_{14}B$ phase (Ref 7, 8).

Nd-Fe-B sintered magnets' coercivity strongly depends on the grain size (Ref 9, 10). Hydrogen–disproportion–desorption recombination (HDDH) and jet milling (JM) applied in the powder making process can control commercial Nd-Fe-B powder size in the 3-5 μm range (Ref 11, 12). However, the grain growth is the most common problem found in sintering. It is well known that the addition of refractory metals, such as Mo, W, Nb, V, or Ta, can significantly suppress grain growth during sintering, due to the grain boundary pinning effect (Ref 13-15). Generally, the relationship between the sintering densification and grain growth is one of the mutual restrictions. During sintering, the relative density increases and the grains grow with the sintering temperature and time. Therefore, lowering the sintering temperature or sintering time without sacrificing the high density of Nd-Fe-B sintered magnets is the key to control the grain growth during sintering.

Hot isostatic pressing (HIP) is a manufacturing process used to produce fully dense parts through the application of high temperature and high gas pressure simultaneously (Ref 16-18). The advantages of the HIP include better chemical homogeneity, fine grain size, full densification, increased materials utilization, and near-net-shape formability (Ref 19, 20). Therefore, HIP is one promising approach to obtain high-density Nd-Fe-B sintered magnets with a high magnetic performance at a relatively low sintering temperature. Although HIP can reduce sintering temperature and improve density, common steel sheaths for HIP sintering are not suitable for Nd-Fe-B sintered magnets. Without a sheath, Nd-rich phases in the magnets would run off under the action of high air pressure during the HIP sintering process, resulting in poor magnetic performance. Therefore, how to achieve sheath protection of magnets is the main key to HIP sintering.

In this paper, HIP was employed to prepare high-performance Nd-Fe-B sintered magnets. Glass was used to form a protective sheath on the surface of magnets. The effects of HIP low-temperature sintering on microstructure and magnetic properties of Nd-Fe-B sintered magnets were systematically investigated. In addition, the mechanism of coercivity enhancement and densification achievement for HIP-sintered magnets was established. To date, only a few related reports have been found in the literature.

2. Experimental Procedure

2.1 Alloy Preparation

The Nd-Fe-B powder (Beijing Zhongke Sanhuan Hi-tech Co., Ltd), with a nominal composition of 32.0Re (Re-Nd, Pr)-

Fang Yang, Haiying Wang, Ce Zhang, and **Zhimeng Guo**, Institute of Advanced Materials and Technology, University of Science and Technology Beijing, Beijing 100083, China; **Li You** and **Yanli Sui**, State Key Laboratory for Advanced Metals and Materials, University of Science and Technology Beijing, Beijing 100083, China; and **Alex A. Volinsky**, Department of Mechanical Engineering, University of South Florida, Tampa, FL 33620. Contact e-mail: yangfang@ustb.edu.cn.

0.3Dy-bal. Fe-1.0B-2.0M (wt.%, M-Cu, Al, Co, Cr), was used as the raw material. After pressing in a magnetic field of 1352 kA/m, the green compacts were pre-sintered at 1173 K for 3 h in vacuum. The pre-sintered samples were separated into three parts. One part was vacuum-sintered at 1123 K for 5 h. The second part was vacuum-sintered at 1318 K for 5 h. The third part was sealed in a glass tube after being subjected to vacuum. The sealed sample was placed in a graphite crucible. Then, the HIP sintering was performed at 1073, 1123, and 1173 K at 150 MPa with 30-min hold time at those temperatures. The HIP cycle consisted of simultaneous application of temperature and pressure at 5 K/min and at 1 MPa/min, respectively. The corresponding preparation process of the HIP samples is shown in Fig. 1. Subsequently, those two parts of as-sintered magnets were annealed at 1103 K for 2 h and again at 768 K for 6 h.

2.2 Testing and Characterization

The magnets were cut into cylinders (8 mm diameter and 5 mm height) and mechanically polished. Five samples for each processing condition were tested to confirm reproducibility. The density of the sintered magnets was determined by the Archimedes' type measurements. The room-temperature magnetic properties of the processed magnets were characterized by a magnetic measurement device (NIM-200C, 0-2.6 T demagnetizing field range). Thermal analysis was performed using differential scanning calorimetry (DSC, NETZSCHSTA449) under Ar protective gas. Phases in the magnets were analyzed by x-ray diffraction (XRD) using the Shimadzu XRD-6000 diffractometer with CuKα radiation operating at 40 kV and 40 mA. Oxygen content in magnets was measured by the infrared absorption method (TCH600). Microstructure studies were conducted by backscattered electron scanning microscopy (FESEM, Supra55). Average grain sizes and grain size distribution were evaluated by the image analysis (UTHSCSA Image Tool).

3. Results and Discussion

The density of the pre-sintered magnets is about 6.5 g/cm^3, nearly 85% dense compared to the theoretical density of 7.65 g/cm^3. The gas absorbed on the surface of powder grains and produced by chemical reactions has been removed during pre-sintering. The softening temperature of the glass is about 773 K. The pre-sintered magnets are covered by the glass fragments, as shown in Fig. 1. During HIP sintering, the molten glass covered the surface of the Nd-Fe-B sintered magnets, forming a glass sheath to prevent the loss of liquid Nd-rich phases. Under the action of the high gas pressure in all directions, the HIP-sintered magnets can achieve high density at the low sintering temperature. Without a protective sheath, the loss of Nd-rich phases will be present due to gas pressure, resulting in the deterioration of sintered density and magnetic performance.

The DSC curve of the Nd-Fe-B sintered magnets is shown in Fig. 2. The DSC analysis was carried out from room temperature to 1323 K, at a constant heating rate of 0.67 K/s. Two exothermic peaks are observed. The first peak, T_{x1}, at 600 K corresponds to the Curie temperature of the $Nd_2Fe_{14}B$ phase. The second peak, T_{x2}, at about 1031 K corresponds to the liquidus temperature of the Nd-Fe-B sintered magnets. The sintering of Nd-Fe-B magnets belongs to liquid phase sintering. During sintering, the liquid Nd-rich phases play a key role in improving the sinterability. The HIP temperature was chosen around the liquidus temperature. Figure 3 presents the magnetic properties of the Nd-Fe-B sintered magnets fabricated by different methods at different sintering temperatures.

The density of all sintered magnets is above 7.55 g/cm^3, except the magnets vacuum-sintered at 1123 K (6.92 g/cm^3), as listed in Table 1. In general, the density of commercial magnets needs to be above 7.5 g/cm^3. When sintered at the same temperature (1123 K), the density of the HIP magnets reached 7.58 g/cm^3, which is the same as the magnets vacuum-sintered

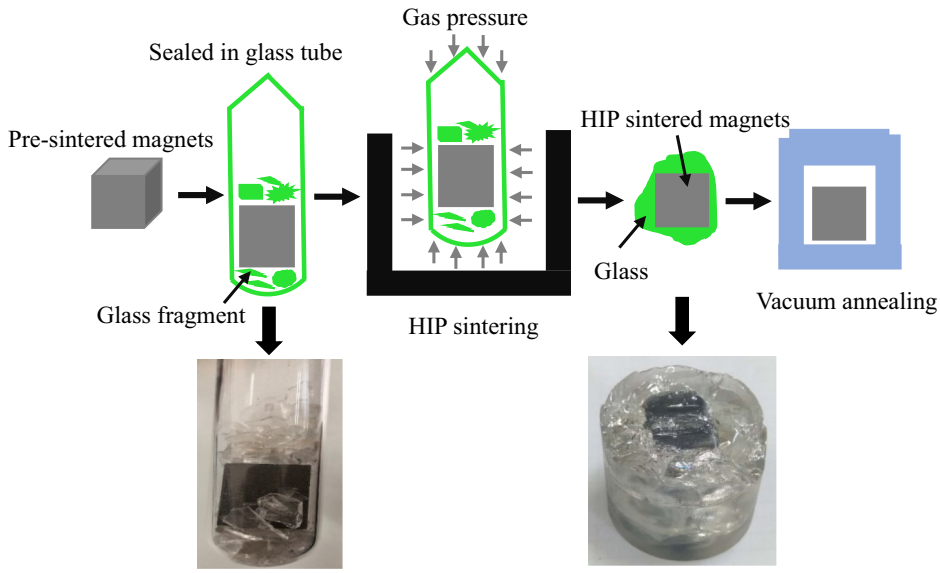

Fig. 1 Process flow diagram of the HIP Nd-Fe-B sintered magnets

at 1318 K, and the relative density is 99%. Therefore, HIP is an effective way to achieve nearly full densification at the low sintering temperature. The measured coercivity H_{cj} and remanence B_r values of the magnets vacuum-sintered at 1318 K are 1067.7 kA/m and 1.292 T, respectively. In the magnets HIP-sintered at 1073 K, the H_{cj} value increased to 1142.5 kA/m. When increasing the HIP sintering temperature to 1123 K, the coercivity reached its maximum value. The coercivity increased to 1238.5 kA/m, and the peak value was 16% higher than the magnets vacuum-sintered at 1318 K. The corresponding B_r decreased to 1.269 T. Upon further increasing the HIP sintering temperature, the coercivity significantly decreased. In conclusion, with the increase in the HIP sintering temperature, the coercivity increased and then decreased, while the remanence decreased, as shown in Fig. 3.

The indices of the crystallographic planes of the $Nd_2Fe_{14}B$ phase in the magnets are labeled in Fig. 4. For the Nd-Fe-B sintered magnets, the main crystallographic planes are (105) and (006). The I(006)/I(105) intensity ratio can represent the orientation degree of the magnets (Ref 21). Compared to the vacuum-sintered magnets, the XRD pattern of the HIP-sintered magnets shows a slight shift. Moreover, the diffraction intensity of the (006) peak significantly reduces, and the intensity of the (105) peak increases accordingly. This means that as the I(006)/I(105) ratio decreases, and so does the orientation degree of the magnets.

The composition of the O element in the Nd-Fe-B magnets was measured. There exists a significant difference between O contents in different magnets. In the magnets vacuum-sintered at 1318 K, the O content is about 4000 ppm. When the magnets were fabricated by HIP, the O content was nearly 4700 ppm. Compared to the magnets vacuum-sintered at 1318 K, the HIP magnets should be slightly oxidized. In addition, the O content in the magnets vacuum-sintered at 1123 K is up to 8800 ppm, which is related to the magnets density (6.92 g/cm^3). The number of pores is relatively high, resulting in the magnets being easily oxidized. For the same reason, due to the low density of the pre-sintered magnets, they are easily oxidized during the sealing process, regardless of their careful protection. Therefore, the O content of the HIP magnets would be relatively higher.

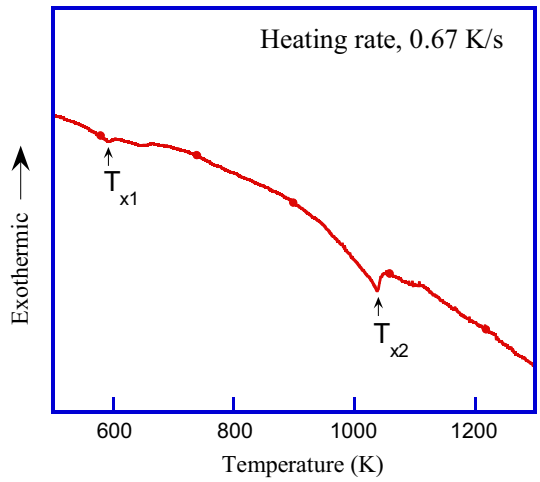

Fig. 2 DSC pattern of Nd-Fe-B sintered magnets

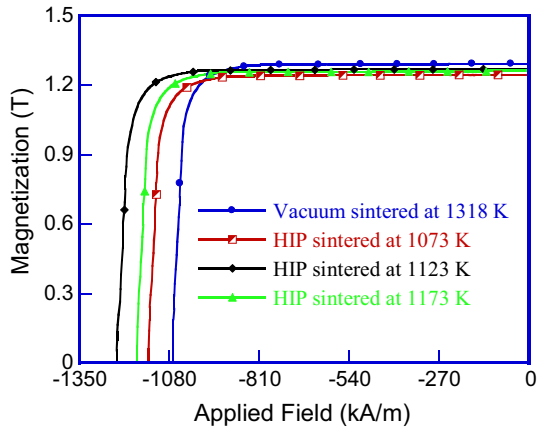

Fig. 3 Demagnetization curves of Nd-Fe-B sintered magnets fabricated by different methods

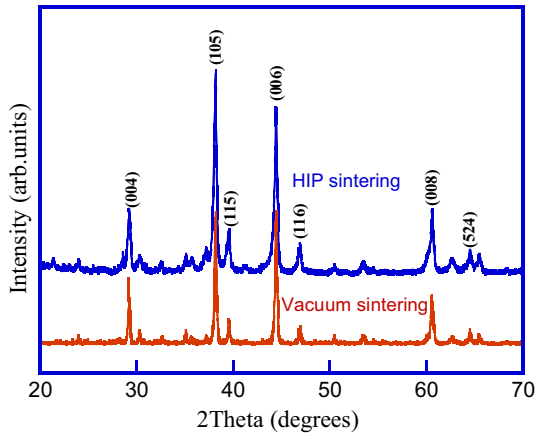

Fig. 4 XRD patterns of Nd-Fe-B sintered magnets fabricated by different methods

Table 1 Density and oxygen content of the Nd-Fe-B magnets fabricated by different methods at different sintering temperatures

	Vacuum		HIP		
Sintering condition	**1123 K**	**1318 K**	**1073 K**	**1123**	**1173**
Density, g/cm^3	6.92	7.58	7.55	7.58	7.60
Relative density, %	90.5	99.1	98.7	99.1	99.3
O content, ppm	8746.4	3986.1	4658.2	4730.7	4701.5

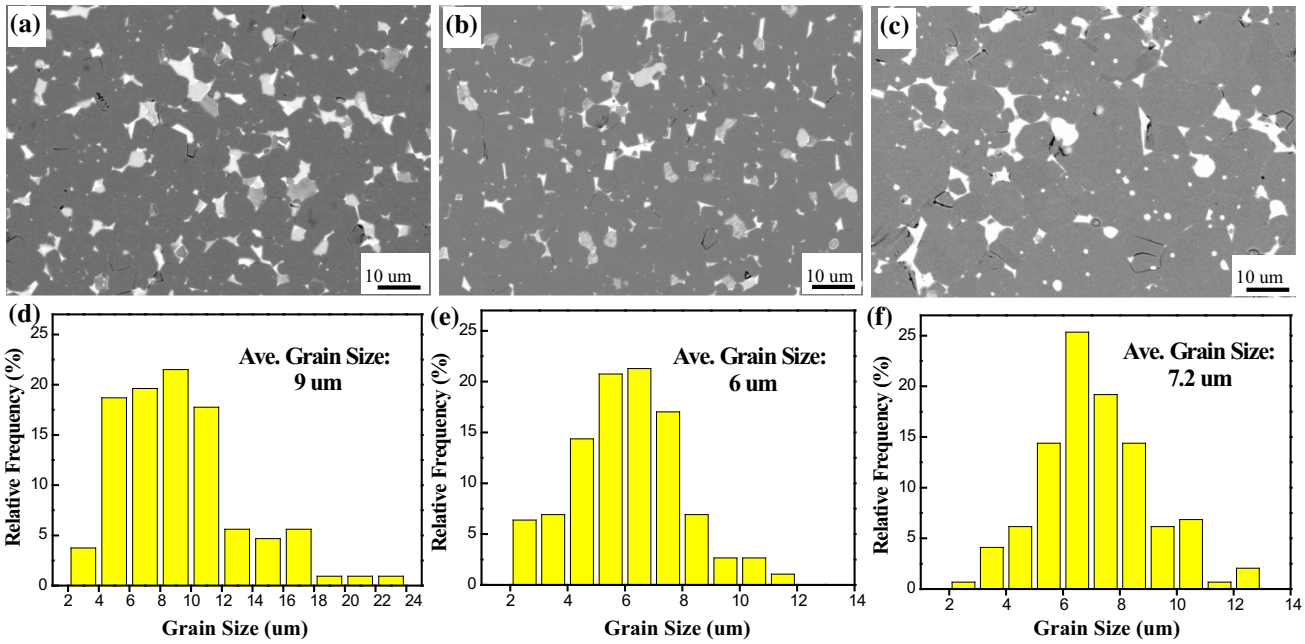

Fig. 5 SEM images and grain size distribution of Nd-Fe-B sintered magnets fabricated by: (a) vacuum sintering at 1318 K, (b) HIP sintering at 1123 K, and (c) HIP sintering at 1173 K

The microstructure changes and grain size distribution of the magnets fabricated by different methods are shown in Fig. 5. The dark regions are the $Nd_2Fe_{14}B$ main phases, and the white regions correspond to the Nd-rich phases. In the vacuum-sintered magnets, the average grain size is 9 μm, as shown in Fig. 5(d). In contrast, the grain size is relatively small and the grain size distribution is more uniform in the HIP-sintered magnets, as shown in Fig. 5(e) and (f). The average grain size of the magnets HIP-sintered at 1123 K is 6 μm, approximately 3 μm smaller than the magnets vacuum-sintered at 1318 K. Therefore, grain refinement is achieved by the HIP low-temperature sintering. As a result, coercivity enhancement of 16% was obtained in the magnets HIP-sintered at 1123 K. Upon further increasing the HIP sintering temperature to 1173 K, the grain growth initiates. The average grain size is 7.2 μm, as shown in Fig. 5(f). HIP sintering at much higher temperature causes grains to grow quickly, which can decrease the coercivity of the magnets.

The above results indicate that the HIP is a promising method to obtain fine grain size in the Nd-Fe-B sintered magnets. Under the action of high gas pressure, the magnets can achieve rapid densification at a relatively low sintering temperature without causing abnormal grain growth. Normally, the vacuum-sintering temperature of the commercial Nd-Fe-B sintered magnets is about 1323 K, and the corresponding sintered density can reach above 7.55 g/cm^3. It is no surprise that the average grain size is relatively large, as shown in Fig. 5(a). Interestingly, when the magnets were fabricated by HIP, the sintering temperature significantly decreased to 1123 K, which is approximately 200 K lower than the vacuum-sintered magnets. The average grain size decreased from 9 to 6 μm. Not only that, but the sintered density also reached 7.58 g/cm^3. Consequently, the coercivity of the HIP-sintered magnets increased from 1067.7 to 1238.5 kA/m, as shown in Fig. 3. It is worth noting that the HIP-sintered magnets have a relatively higher O content of 4700 ppm. This was the main cause for lower remanence seen in Fig. 3; however, the decrease is relatively small. As already mentioned, the relative density of the pre-sintered magnets is only 85%, and they can easily suffer from oxidation when exposed to oxygen. During the sealing process, the pre-sintered magnets may have been lightly oxidized, although the experimental process was strictly controlled. Compared to the magnets vacuum-sintered at 1318 K, the remanence of the magnets HIP-sintered at 1123 K decreased from 1.292 to 1.269 T. As to the low orientation degree of HIP magnets, it may be caused by the high air pressure on the magnets. Therefore, the next step is to focus on studying the effects of pre-sintering and air pressure on magnetic properties and the orientation degree of the HIP magnets.

4. Conclusions

In summary, microstructure and magnetic properties of the Nd-Fe-B sintered magnets fabricated by HIP were explored. Grain refinement was achieved by HIP low-temperature sintering, resulting in the coercivity enhancement. The sintering temperature was significantly decreased by about 200 K. The optimal HIP sintering temperature was about 1123 K. On the one hand, the sintered density reached 7.58 g/cm^3, which is same as the magnets vacuum-sintered at 1318 K. On the other hand, the average grain size was 6 μm, which was approximately 3 μm smaller compared to vacuum-sintered magnets. Coercivity enhancement of 16% was obtained in the magnets HIP-sintered at 1123 K because of the smaller grain size. Upon further increasing the HIP sintering temperature, the deterioration of magnetic properties was correlated with the grain growth.

Acknowledgments

This work was supported by the State Key Laboratory of Advanced Metals and Materials (No. 2018-Z06).

References

1. K. Hono and H. Sepehri-Amin, Strategy for High-Coercivity Nd-Fe-B Magnets, *Scripta Mater.*, 2012, **67**, p 530–535
2. K. Loewe, C. Brombacher, M. Katter, and O. Guttfleisch, Temperature-Dependent Dy Diffusion Processes in Nd-Fe-B Permanent Magnets, *Acta Mater.*, 2015, **83**, p 248–255
3. K.C. Lu, X.Q. Bao, M.H. Tang, G.X. Chen, X. Mu, J.H. Li, and X.X. Gao, Boundary Optimization and Coercivity Enhancement of High (BH)max Nd-Fe-B Magnet by Diffusing Pr-Tb-Cu-Al Alloys, *Scripta Mater.*, 2017, **138**, p 83–87
4. T.G. Woodcock and O. Gutfleisch, Multi-phase EBSD Mapping and Local Texture Analysis in NdFeB Sintered Magnets, *Acta Mater.*, 2011, **59**, p 1026–1036
5. W.F. Li, H. Sepehri-Amin, T. Ohkubo, N. Hase, and K. Hono, Distribution of Dy in High-Coercivity (Nd, Dy)-Fe-B Sintered Magnet, *Acta Mater.*, 2011, **59**, p 3061–3069
6. T.H. Kim, S.R. Lee, H.J. Kim, M.W. Lee, and T.S. Jang, Simultaneous Application of Dy-X (X = F or H) Powder Doping and Dip-Coating Processes to Nd-Fe-B Sintered Magnets, *Acta Mater.*, 2015, **93**, p 95–104
7. J. Liu, H. Sepehri-Amin, T. Ohkubo, K. Hioki, A. Hattori, T. Schrefl, and K. Hono, Grain Size Dependence of Coercivity of Hot-Deformed Nd-Fe-B Anisotropic Magnets, *Acta Mater.*, 2015, **82**, p 336–343
8. W.F. Li, A.M. Gabay, M. Marinescu-Jasinski, J.F. Liu, C. Ni, and G.C. Hadjipanayis, Microstructure of Sintered ND-Fe-Ga-B Magnets with Mo and MoS_2 Addition, *J. Magn. Magn. Mater.*, 2012, **324**, p 1391–1396
9. K. Uestuener, M. Katter, and W. Rodewald, Dependence of the Mean Grain Size and Coercivity of Sintered Nd-Fe-B Magnets on the Initial Powder Particle Size, *IEEE Trans. Magn.*, 2006, **42**(10), p 2897–2899
10. W.F. Li, T. Ohkubo, K. Hono, and M. Sagawa, The Origin of Coercivity Decrease in Fine Grained Nd-Fe-B Sintered Magnets, *J. Magn. Magn. Mater.*, 2009, **321**, p 1100–1105
11. H. Sepehri-Amin, T. Ohkubo, K. Hono, K. Guth, and O. Gutfleisch, Mechanism of the Texture Development in Hydrogen-Disproportionation-Desorption-Recombination (HDDR) Processed Nd-Fe-B Powders, *Acta Mater.*, 2015, **85**, p 42–52
12. F. Bittner, T.G. Woodcock, L. Schultz, C. Schwobel, O. Gutfleisch, G.A. Zickler, J. Fidler, K. Ustuner, and M. Katter, Normal and Abnormal Grain Growth in Fine-Grained Nd-Fe-B Sintered Magnets Prepared from He Jet Milled Powders, *J. Magn. Magn. Mater.*, 2017, **426**, p 698–707
13. J.W. Kin, W.S. Lee, J.M. Byun, S.H. Kim, and Y.D. Kim, Grain Refinement in Heavy Rare Earth Element-Free Sintered Nd-Fe-B Magnets by Addition of a Small Amount of Molybdenum, *J. Appl. Phys.*, 2015, **117**, p 17B523
14. W.H. Cheng, W. Li, C.J. Li, and X.M. Li, The Role of Nb Addition in Nd-Fe-B Sintered Magnets with High Performance, *J. Alloys Compd.*, 2001, **319**, p 280–282
15. T.Y. Chu, T.S. Chin, C.H. Lin, and J.M. Yao, Evidence of Domain-Wall Pinning in W-Doped (NdDy)(FeCo)B Sintered Magnets, *J. Appl. Phys.*, 1994, **76**, p 6834–6836
16. K. Essa, P. Jamshidi, J. Zou, M.M. Attallah, and H. Hassanin, Porosity Control in 316L Stainless Steel Using Cold and Hot Isostatic Pressing, *Mater. Des.*, 2018, **138**, p 21–29
17. T. Yildiz, N. Kati, and A.K. Gur, The Effect of Sintering Temperature on Microstructure and Mechanical Properties of Alloys Produced by Using Hot Isostatic Pressing Method, *J. Alloys Compd.*, 2018, **737**, p 8–13
18. H.V. Atkinson and S. Davies, Fundamental Aspects of Hot Isostatic Pressing: An Overview, *Metall. Mater. Trans. A*, 2000, **31A**, p 2981–3000
19. S. Irukuvarghula, H. Hassanin, C. Cayron, M.M. Attallah, D. Stewart, and M. Preuss, Evolution of Grain Boundary Network Topology in 326L Austenitic Stainless Steel During Powder Hot Isostatic Pressing, *Acta Mater.*, 2017, **133**, p 269–281
20. J.L. Sulley, B.K. Bull, and A.C. Wood, Hot Isostatic Pressing of Large Bore, Stainless Steel Pipework for a Safety Critical Application, *Adv. Mater. Res.*, 2012, **378**, p 752–758
21. W.J. Mo, L.T. Zhang, A.D. Shan, L.J. Cao, J.S. Wu, and M. Komuro, Microstructure and Magnetic Properties of NdFeB Magnet Prepared by Spark Plasma Sintering, *Intermetallics*, 2007, **15**, p 1483–1488